# ANN-BASED SURFACE ROUGHNESS MODELLING OF AA7075-T6 SLOT MILLING: CUTTING TECHNIQUE EVALUATION

**Anastasios TZOTZIS[1], Apostolos KORLOS[2], Rajesh Kumar VERMA[3] and Panagiotis KYRATSIS[1]**

*[1] University of Western Macedonia, Product and Systems Design Engineering Department, Kila Kozani, 50100 Greece, E-mail: a.tzotzis@uowm.gr, pkyratsis@uowm.gr*

*[2]International Hellenic University, Industrial Engineering and Management Department, Sindos Thessaloniki, 57400, Greece, E-mail: apkorlos@ihu.gr*

*[3]Harcourt Butler Technical University, Department of Mechanical Engineering, Kanpur (U.P.), 208002, India, E-mail: rkvme@hbtu.ac.in*

***ABSTRACT:*** *Surface roughness is considered to be an index of a part's machined surface quality and thus it is widely used in the industry to evaluate both the machinability of a material and the performance of a cutting process. The current article, presents an investigation on the surface quality evaluation of 7075-T6 aluminium alloy (AA) slot milling with both up-milling and down-milling techniques, by utilizing carbide end mills. Moreover, the study includes the modelling procedure of the process, according to the artificial neural network (ANN) methodology. The study revealed that both cutting techniques performed equally, with a mean value of surface roughness close to 0.8422μm for up-milling and 0.8396μm for down-milling respectively. In addition, both up-milling and down-milling ANN models yielded predictions very close to the experimental results with relative error varying between −13.68% and 15.71%. Concluding, the mean effects plots were employed to visualize the effect of each one of the three cutting parameters (spindle speed, feed and cutting depth) that were applied to the experiments, on the arithmetic mean value of surface roughness (Ra). It was found that both feed and depth of cut act increasingly on the surface roughness, whereas any increase in spindle speed generates the opposite result.*

***KEYWORDS****: AA7075, ANN, Slot Milling, Surface Roughness, Surface Quality, Up-milling, Down-milling*

## 1 INTRODUCTION

Aluminium alloy 7075 (AA) can be heat-treated, yielding this way an alloy much stronger than carbon steel. Therefore, it is widely used in aerospace and applications, where a high strength-to-weight ratio is mandatory. One of the most important parameters studied during the machining of AAs, is the surface quality in terms of surface roughness.

Subramanian et al. [1] studied the influence of typical cutting parameters, as well as tool geometric aspects, on the generated surface roughness during the end milling process of AA7075-T6. Moreover, the authors modelled the process by using the Response Surface Methodology (RSM). Yasar [2] utilized a combination of the Finite Element Method (FEM) and Gray Relational Analysis (GRA) for the optimization of the AA7075 surface roughness during drilling, in addition to other important cutting parameters. Garcia-Jurado et al. [3] examined the surface roughness in dry turning of A92024 AA, by analyzing the adhesion tool wear effects. Vakondios et al [4] studied the effects of different milling strategies on the produced surface quality, in ball end milling of AA7075-T6. An example study of the AA1100 micro-milling is the one by Kiswanto et al. [5]. The authors investigated the influence of the spindle speed, feed rate and machining time on the generated surface roughness and burr formation. Taguchi and regression methods complement the aforementioned methodologies and techniques in the surface roughness evaluation topic. Durakbasa et al. [6] utilized similar methods for the assessment of the surface roughness during AA7075 milling. The study presented modelling of the process with respect to the used tool cutting edge radius, geometry and standard machining conditions. A number of studies [7, 8] that exist in the literature related to AA7075 machining support the significance of the specific alloy.

With the number of the AAs that are available worldwide in mind, as well as the significance of the specific aluminium temper, the present paper aims to contribute towards the examination of the AA7075-T6 surface quality generated during the slot milling process. Moreover, it provides insight on the performance of the two typical milling methods, up-milling and down-milling. Finally, this study presents a model of the process, based on the Artificial Neural Network (ANN) method. Despite the fact that surface roughness has been widely studied for different materials with well-established tools and methods, ANN is considered to be a more sophisticated method compared to traditional statistical methods, yielding reliable results of high accuracy.

## 2 MATERIALS AND METHODS

### 2.1 Experimental testing

Two sets of 27 slot milling tests each, were performed to evaluate the selected strategies, up-milling and down-milling. The cutting tests were carried out with a vertical milling machine, according to the full factorial design, which comprises of three cutting parameters at three value levels. Table 1 shows the selected cutting conditions and the corresponding levels. Spindle speed, feed and cutting depth are considered to be standard parameters when dealing with milling and therefore they were chosen for this study. The equivalent values can be found in the manufacturer's catalogue, being the recommended ones for the machining of aluminium. Specifically, the test material was AA7075-T6. Table 2 presents the most important mechanical properties of the selected temper. Two plates of similar dimensions, served as the workpieces.

**Table 1. The machining parameters**

| Levels | S (min−1) | Vf (mm/min) | ap (mm) |
|---|---|---|---|
| 1 | 710 | 56 | 1 |
| 2 | 1000 | 80 | 2 |
| 3 | 1400 | 112 | 3 |

**Table 2. AA7075-T6 material properties [9]**

| E (GPa) | ρ (kg/m3) | ν | Ultimate tensile strength (MPa) | Yield tensile strength (MPa) |
|---|---|---|---|---|
| 71.7 | 2,810 | 0.33 | 560 | 480 |

Finally, Figure 1a depicts a sample series of nine cuts during down-milling, whereas Figure 1b illustrates the measurement procedure for the slots generated with the up-milling technique at 1000min$^{-1}$. The complete results of both sets are presented in Table 3, according to the applied cutting conditions.

Surface roughness was the investigated output parameter of the study, since it is a widely studied index of surface quality. To measure surface roughness, DIAVITE DH-8 roughness gauge was utilized. Each slot was measured at three specific points, equally distributed on the slot length and then the mean value was calculated. Hence, a total of 162 measurements were performed. The arithmetic mean ($R_a$) was selected as the surface roughness parameter for comparison, since it is considered to be an effective to evaluate surface roughness [10].

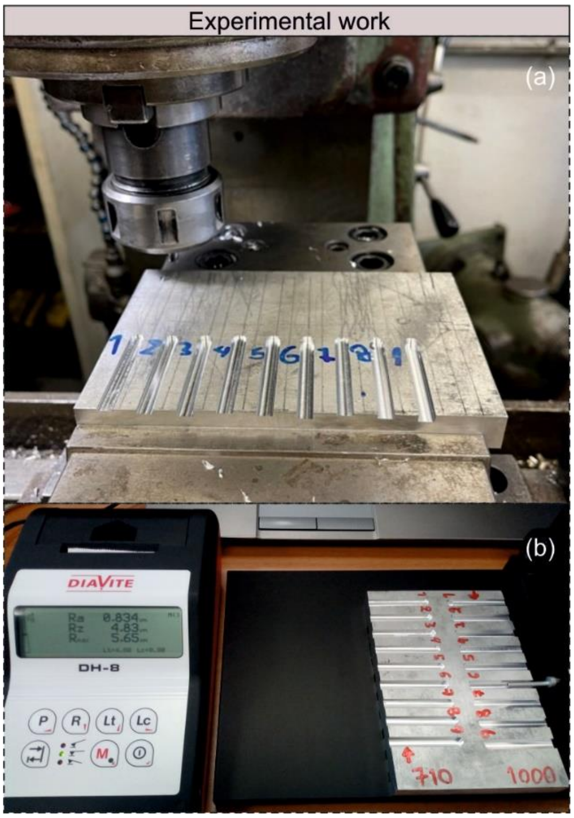


**Fig. 1. Sample cutting test (a) and surface roughness measurement (b).**

| Catalogue number | $D$ (mm) | $l$ (mm) | Corner chamfer (mm) | $z$ |
|---|---|---|---|---|
| 19992 6.000 | 6 | 13 | 0.090 | 3 |

**Fig. 2. The machine tool characteristics**

To perform the cuts, 54 identical tools were used. Each one performed a single cutting test, creating a slot with length equal to 45mm. Figure 2 illustrates the used tool, as well as includes the typical geometrical characteristics of the end-mill. The tool catalogue number is 19992 6.000, which corresponds to 45° chamfered end mills, ideal for slotting, with *z*=3, flute helix angle 45°, shank diameter equal to 6mm with e8 tolerance grade and effective cutting length 13mm.

**Table 3. The experimental tests and results**

| | **Input** | | | **Output** | |
|---|---|---|---|---|---|
| **Test number** | **S (min−1)** | **Vf (mm/min)** | **ap (mm)** | **Ra (µm) up-milling** | **Ra (µm) down-milling** |
| **1** | 710 | 56 | 1 | 0.595 | 0.671 |
| **2** | 710 | 56 | 2 | 0.790 | 0.783 |
| **3** | 710 | 56 | 3 | 0.828 | 0.913 |
| **4** | 710 | 80 | 1 | 0.880 | 0.957 |
| **5** | 710 | 80 | 2 | 1.008 | 0.918 |
| **6** | 710 | 80 | 3 | 0.975 | 0.977 |
| **7** | 710 | 112 | 1 | 0.908 | 0.837 |
| **8** | 710 | 112 | 2 | 1.294 | 1.226 |
| **9** | 710 | 112 | 3 | 1.207 | 0.918 |
| **10** | 1000 | 56 | 1 | 0.676 | 0.727 |
| **11** | 1000 | 56 | 2 | 0.851 | 0.627 |
| **12** | 1000 | 56 | 3 | 0.942 | 0.744 |
| **13** | 1000 | 80 | 1 | 0.781 | 0.817 |
| **14** | 1000 | 80 | 2 | 0.791 | 0.939 |
| **15** | 1000 | 80 | 3 | 0.884 | 0.818 |
| **16** | 1000 | 112 | 1 | 0.821 | 0.944 |
| **17** | 1000 | 112 | 2 | 0.919 | 1.094 |
| **18** | 1000 | 112 | 3 | 1.178 | 1.029 |
| **19** | 1400 | 56 | 1 | 0.690 | 0.703 |
| **20** | 1400 | 56 | 2 | 0.796 | 0.739 |
| **21** | 1400 | 56 | 3 | 0.697 | 0.627 |
| **22** | 1400 | 80 | 1 | 0.696 | 0.667 |
| **23** | 1400 | 80 | 2 | 0.703 | 0.843 |
| **24** | 1400 | 80 | 3 | 0.690 | 0.789 |
| **25** | 1400 | 112 | 1 | 0.549 | 0.803 |
| **26** | 1400 | 112 | 2 | 0.743 | 0.783 |
| **27** | 1400 | 112 | 3 | 0.847 | 0.776 |

## 2.2 ANN-based modelling

A number of studies related to manufacturing processes [11–13] and especially to the surface roughness evaluation, reveal the robustness of the ANN modelling. This study utilizes a network according to the feedforward, backpropagation method, since it is the most used method in problems, where non-linear parameters are involved. This method intends to minimize the difference between the actual and the net output of the network, by continuously adjusting the weights of the linkages. The algorithm serving this purpose was proposed by Levenberg and Marquardt [14]. For both experimental sets, the obtained data were divided into three groups. One group, containing 70% of the data, was used for the training of the model, another group with 15% of the data, for validation and the last one, for the model testing. The number of the neurons and the structure of the network were determined by means of trial and error. A number of runs were performed by utilizing neurons between 6 and 12 and the correlation value *R* was recorded. Table 4 includes the recorded values. Therefore, the 3-10-1 ANN structure was selected for both up-milling and down-milling models, according to the three input variables, ten hidden neurons and one output. The network structure used in the presented models is illustrated in Figure 3.

**Table 4. The results of the ANN structure trials**

| Structure | R-value for Ra | |
|---|---|---|
| | **up-milling** | **down-milling** |
| 3-6-1 | 0.93817 | 0.94520 |
| 3-7-1 | 0.95710 | 0.91554 |
| 3-8-1 | 0.95601 | 0.95722 |
| 3-9-1 | 0.93984 | 0.94657 |
| 3-10-1 | 0.99065 | 0.96931 |
| 3-11-1 | 0.95114 | 0.96698 |
| 3-12-1 | 0.95274 | 0.90041 |

The hyperbolic tangent (tanh) transfer function was used in the developed model as the activation function, since it allows for a simplified mapping of the output (negative, neutral or positive), which in addition enables the centering of the data, facilitating this way the learning process. In the present models, the data were normalized between [−1, 1], in order to tackle any performance issues. Eq. 1 describes the applied activation function, whereas Eq. 2 expresses the result for the output variables, adjusted for the summation of the weighted data. Where *z* represents the output variable, $R_a$, $W_i$ are the output layer weights for *n* hidden nodes, *f*(*x*) is the hyperbolic tangent activation function, for each numerical value of the hidden neurons $H_i$, and finally *b* is the bias of the output layer.

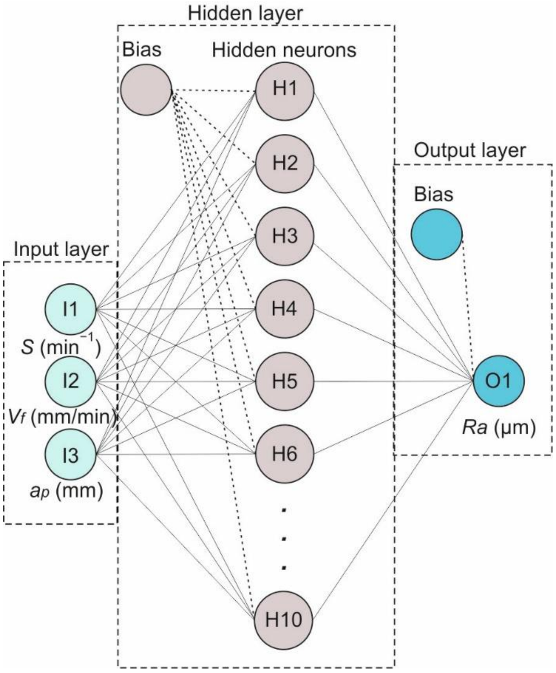


**Fig. 3. The ANN structure of the study**

$$f(x) = \tanh(x) = \frac{2}{1-e^{-2x}} - 1 \tag{1}$$

$$z = \sum_{i=1}^{n} W_i f(H_i) + b \tag{2}$$

The normalization process of both the input and the output data, according to the activation function's range, was carried out with the aid of the next formulas. Eq. 3 was used for the normalization of the input parameter or target result $y_{normalized}$, as a function of the actual input or target result *y* in accordance to the normalization coefficients *α* and *β*, which can be calculated with Eq. 4 and 5 respectively. Where $y_{max}$ and $y_{min}$ are the maximum and minimum actual value of the input or target data accordingly. This process is especially useful when the input data levels are not symmetrical (i.e. 56mm/min, 80mm/min and 112mm/min). In addition, it should be noted that the normalized data, must be denormalized with the same procedure after the training is complete, to acquire the actual output results.

$$y_{normalized} = \alpha \times y + \beta \tag{3}$$

$$\alpha = \frac{2}{y_{\max} - y_{\min}} \tag{4}$$

$$\beta = -\frac{y_{\max} + y_{\min}}{y_{\max} - y_{\min}} \tag{5}$$

The calculation matrices that are required to determine the arithmetic values of each one of the hidden neurons $H_i$, according to the generated weights of the input layer and the hidden layer biases, are represented by Eq. 6 and 7. Furthermore, the weights and biases of the output layer that were used with Eq. 2 are shown in Table 5.

$$\begin{bmatrix} H_1 \\ H_2 \\ H_3 \\ H_4 \\ H_5 \\ H_6 \\ H_7 \\ H_8 \\ H_9 \\ H_{10} \end{bmatrix} = \begin{bmatrix} 3.066 & -2.6142 & -0.86483 \\ 0.89684 & 0.92315 & -1.8187 \\ -2.7146 & 1.9646 & 1.3079 \\ 1.1971 & 0.22006 & 2.1935 \\ -0.39937 & 1.9919 & 1.7155 \\ -0.24489 & -2.7713 & 1.8474 \\ -2.8122 & 0.070674 & 1.7446 \\ 0.72359 & 2.2655 & -1.8188 \\ 2.4726 & 2.3818 & 0.30583 \\ 2.6443 & 1.0176 & -0.89901 \end{bmatrix} \times \begin{bmatrix} S \\ V_f \\ a_p \end{bmatrix} + \begin{bmatrix} -1.9661 \\ -2.9796 \\ 1.6644 \\ -0.91465 \\ 0.63965 \\ 0.29671 \\ -2.5634 \\ 0.36108 \\ 1.9932 \\ 2.9991 \end{bmatrix} \tag{6}$$

$$\begin{bmatrix} H_1 \\ H_2 \\ H_3 \\ H_4 \\ H_5 \\ H_6 \\ H_7 \\ H_8 \\ H_9 \\ H_{10} \end{bmatrix} = \begin{bmatrix} -0.81858 & -1.3119 & -2.2417 \\ 1.5566 & 2.1475 & -1.9342 \\ 2.6368 & -1.5959 & 0.73122 \\ -2.3545 & -1.736 & 0.83881 \\ -2.4577 & 0.73139 & -1.3059 \\ 1.7097 & 0.87789 & 1.7732 \\ -0.1649 & 2.1938 & -2.3063 \\ 1.1231 & -1.3642 & 2.4258 \\ -1.4191 & -2.5052 & -2.6118 \\ -3.2361 & 0.89192 & -0.24941 \end{bmatrix} \times \begin{bmatrix} S \\ V_f \\ a_p \end{bmatrix} + \begin{bmatrix} 3.1486 \\ -2.1219 \\ -1.1216 \\ 1.1848 \\ 0.71824 \\ 0.082224 \\ -1.66 \\ 1.7439 \\ -1.6355 \\ -2.5733 \end{bmatrix} \tag{7}$$

**Table 5. The weights and biases of the model**

| | | | | | | |
|---|---|---|---|---|---|---|
| **z = Ra up-milling** | W1 | W2 | W3 | W4 | W5 | W6 |
| | 1.2353 | −0.94707 | 1.4553 | −0.040083 | −0.21114 | −0.31758 |
| | W7 | W8 | W9 | W10 | b | |
| | 1.4739 | −0.091089 | 0.12459 | 1.2896 | −1.1776 | |
| **z = Ra down-milling** | W1 | W2 | W3 | W4 | W5 | W6 |
| | 0.093285 | −1.3191 | −0.65406 | −0.69848 | −0.30512 | −0.47258 |
| | W7 | W8 | W9 | W10 | b | |
| | 1.018 | 0.49829 | −0.56883 | 0.18604 | −0.9487 | |

The regression plots for both up-milling model and down-milling are illustrated in Figure 4a and 4b respectively. The goodness of fit between the experimental and the predicted values is evident on both plots, since the predicted data points are very close to the zero-error line, represented by the dashed line. Furthermore, the correlation values for training, validation and testing, verify the high level of accuracy, suggesting that acceptable error values are expected by the model prediction.

## 3 RESULTS

### 3.1 Surface roughness assessment

To assess the surface quality of the machined aluminium plates, the surface roughness was measured with the gauge as described in section 2.1. The calculated mean values were then imported to a spreadsheet software in order to examine the performance between the two compared milling methods. The comparison is graphically illustrated in Fig. 5. In general, both methods performed approximately the same. However, the mean value for all 27 experiments carried out with the up-milling method, was calculated equal to 0.8422μm, whereas with the down-milling method, was found to be 0.8397μm. In terms of the spindle speed, the feed and the cutting depth, the generated effects of their means were plotted in the graphs of Fig. 6. The main effects plot is an effective tool when considering the differences between the level means for a variety of cutting parameters [9, 15].

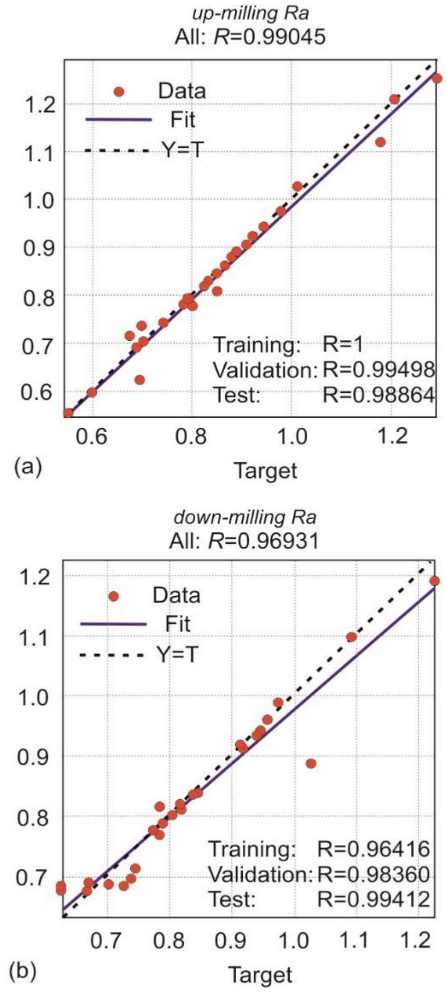


**Fig. 4. The regression plots of the model: for up-milling (a) and down-milling (b)**

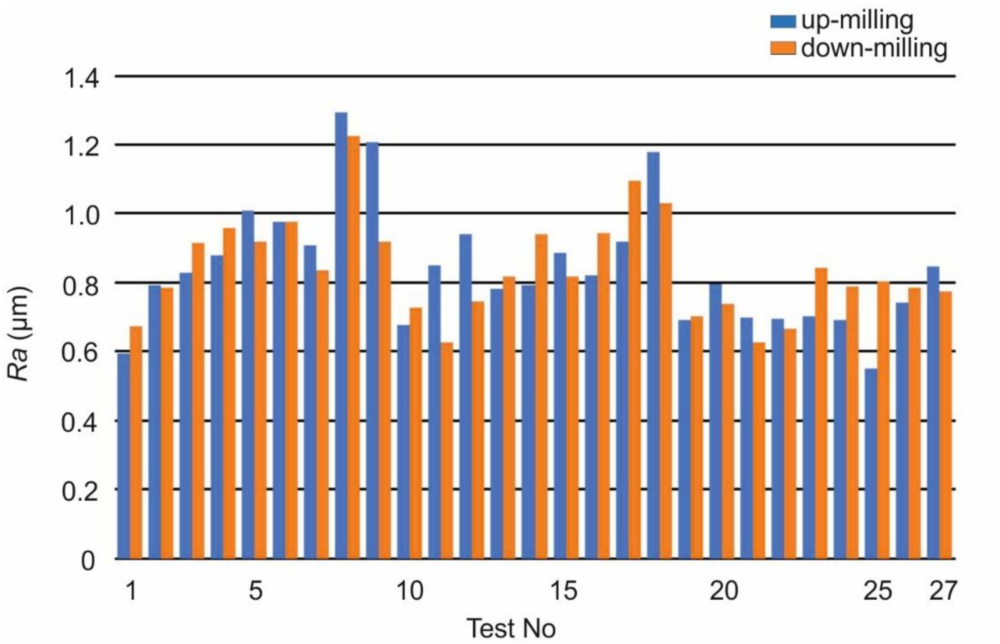


**Fig. 5. Comparison graph between the up-milling and the down-milling method**

Figure 6a illustrates the main effects plot for up-milling, whereas Figure 6b for down-milling. Observation of the plots led to the following conclusions. First, it is evident that an increase in the spindle speed, acts decreasingly on the produced surface roughness for both milling methods. Especially, spindle speed equal to 1400min$^{-1}$, is responsible for the achievement of very low surface roughness.

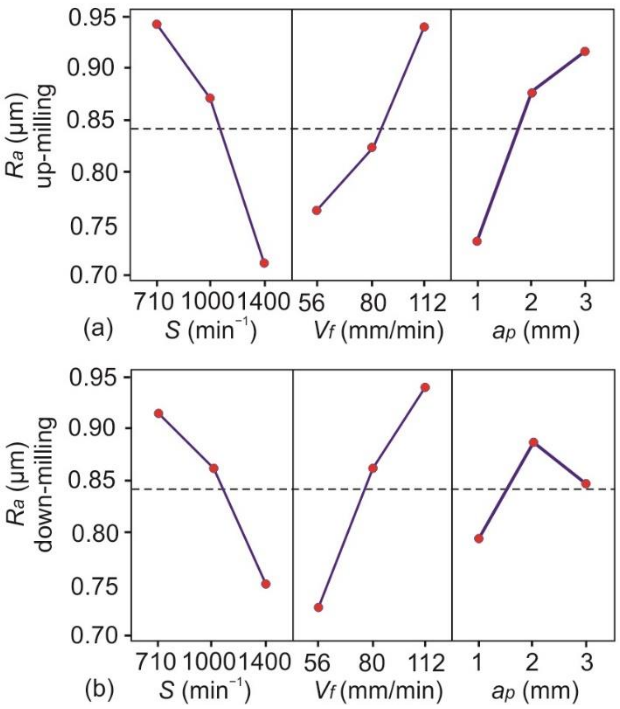


**Fig. 6 The regression plots of the model: for up-milling (a) and down-milling (b)**

This scheme is visible on both up-milling and down-milling techniques. On the contrary, higher feed values generate surface of lower quality. Moreover, down-milling seems to benefit from the feed value of 56mm/min. Finally, the increasing of depth of cut produces higher values of surface roughness. However, this increase declines after the 2mm depth of cut. Especially during down-milling, the decline is considerable. Similar results were reported in the study [16] related to slot milling of AISI-H13 steel, especially on the effects induced by the feed and the depth of cut.

## 3.2 Model evaluation

The output of the ANN models was used for the comparison between the test results and the simulated values of roughness. The evaluation of the model prediction capacity was carried out with the mean absolute percentage error (MAPE). The absolute value of each error was estimated and then the mean value of the summation of the errors was obtained. Table 6 includes all computed absolute error values, as well as the MAPE for both cases. Considering the wide range of the machining conditions that the study covers, the MAPEs can be considered very low and thus both models exhibit very good correlation levels with the experimental output data. The MAPE for the up-milling method was found to be 2.67%, and for down-milling 2.54%. This fact strengthens the statement that both models performed well in terms of their prediction abilities, are sufficiently fit and can be safely used for prediction purposes within the aforementioned limits.

**Table 6. Error data for the developed ANN models**

| Test | Absolute percentage error | |
|---|---|---|
| | up-milling | down-milling |
| 1 | 0.19 | 2.51 |
| 2 | 10.58 | 1.37 |
| 3 | 0.07 | 0.46 |
| 4 | 0.89 | 0.30 |
| 5 | 0.13 | 1.00 |
| 6 | 0.08 | 1.03 |
| 7 | 0.12 | 0.10 |
| 8 | 1.71 | 2.96 |
| 9 | 6.05 | 0.56 |
| 10 | 0.41 | 5.76 |
| 11 | 0.12 | 8.38 |
| 12 | 0.23 | 4.66 |
| 13 | 0.33 | 0.27 |
| 14 | 0.73 | 0.65 |
| 15 | 15.71 | 0.33 |
| 16 | 11.34 | 0.28 |
| 17 | 0.09 | 0.53 |
| 18 | 0.23 | 13.68 |
| 19 | 0.34 | 2.18 |
| 20 | 7.94 | 5.86 |
| 21 | 0.38 | 9.21 |
| 22 | 0.68 | 1.20 |
| 23 | 0.45 | 0.53 |
| 24 | 12.21 | 0.28 |
| 25 | 0.43 | 0.02 |
| 26 | 0.29 | 4.34 |
| 27 | 0.24 | 0.18 |
| MAPE | 2.67 | 2.54 |

## 3.3 Model validation

The reliability of the two models was examined by performing three extra experiments for each milling method, under arbitrarily selected machining conditions from within the range of the study. The setup of the extra experiments, as well as the results and comparison with the predicted values are presented in Table 7. Despite the fact that the down-milling method exhibits higher values of relative error compared to the up-milling method, fact that is probably related to the lower correlation coefficient of the model, in general the reasonable calculated relative error between the ANN-based predicted values and the experimental results, prove the reliability of the models, as well as the robustness of the ANN method. Consequently, it is safe to assume that both models can be used to predict the surface roughness for any combination of the three applied parameters (spindle speed, feed and cutting depth), within the range of the study.

Table 7. The setup of confirmation tests and the results

| Test No | S (min−1) | Vf (mm/min) | ap (mm) | up-milling | | | down-milling | | |
|---|---|---|---|---|---|---|---|---|---|
| | | | | Simulated Ra (μm) | Experimental Ra (μm) | Relative error % | Simulated Ra (μm) | Experimental Ra (μm) | Relative error % |
| 1 | 900 | 106 | 1.6 | 0.9237 | 0.9450 | −2.25 | 1.1330 | 1.0440 | 8.52 |
| 2 | 1100 | 64 | 2.4 | 0.9230 | 0.8967 | 2.93 | 0.7184 | 0.8167 | −12.04 |
| 3 | 1200 | 92 | 1.2 | 0.6445 | 0.7256 | −11.18 | 0.9640 | 0.8637 | 11.61 |

## 4 CONCLUDING REMARKS

In the present study, an experimental comparison was carried out between the up-milling and down-milling cutting method during machining of AA7075-T6, with carbide flat end-mills. Furthermore, two ANN models were developed for the prediction of the surface roughness, one for each cutting method. In terms of the cutting strategy evaluation, both methods performed well, yielding surface roughness values relatively low for the machining process of aluminium. A mean value of 0.8422μm was calculated for up-milling and 0.8396μm for down-milling respectively, with regard to the total number of the experiments. Moreover, the investigation on the effects of the cutting parameters with respect to the generated roughness, revealed that higher values of spindle speed reduce the surface roughness. In contrast, shifting the feed increases the surface roughness. Finally, the depth of cut exhibited slightly different influence pattern compared to the other two parameters. Specifically, deeper cuts produce more rough surfaces. However, the increase in surface roughness seems to diminish as the depth of cut passes the 2mm limit. In addition, it should be noted that all three machining conditions have a strong effect on the generated roughness.

The computed relative error between the simulated and the experimental values, proved both the reliability and robustness of the developed ANN models, within the scope of the study. For up-milling it was found to be between −11.34% 15.71%, whereas for down-milling between −13.68% and 9.21%.

Since surface roughness is a parameter with strong significance in the industry, future work could possibly include comparison between a number of modern analysis methods such as fuzzy logic, Bayesian neural networks and deep learning.

## 5 ACKNOWLEDGEMENTS

The authors would like to thank Mr. Fotis Ouzounis for his valuable assistance with the realization of the experimental work.

## 6 REFERENCES

1. Subramanian M, Sakthivel M, Sudhakaran R (2014) Modeling and Analysis of Surface Roughness of AL7075-T6 in End Milling Process Using Response Surface Methodology. Arab J Sci Eng 39:7299–7313. https://doi.org/10.1007/s13369-014-1219-z

2. Yaşar N (2019) Thrust force modelling and surface roughness optimization in drilling of AA-7075: FEM and GRA. J Mech Sci Technol 33:4771–4781. https://doi.org/10.1007/s12206-019-0918-5

3. Garcia-Jurado D, Vázquez-Martinez JM, Gámez AJ, et al (2017) Analysis of secondary adhesion tool wear effects on surface roughness in dry turning process of UNS A92024 aluminium alloy. Int J Mechatronics Manuf Syst 10:23–39

4. Vakondios D, Kyratsis P, Yaldiz S, Antoniadis A (2012) Influence of milling strategy on the surface roughness in ball end milling of the aluminum alloy Al7075-T6, Measurement 45:1480-1488

5. Kiswanto G, Zariatin DL, Ko T. J (2014) The effect of spindle speed , feed-rate and machining time to the surface roughness and burr formation of Aluminum Alloy 1100 in micro-milling operation. J Manuf Process 16:435–450. https://doi.org/10.1016/j.jmapro.2014.05.003

6. Durakbasa MN, Akdogan A, Vanli AS, Günay A (2014) Surface Roughness Modeling with Edge Radius and End Milling Parameters on Al 7075 Alloy Using Taguchi and Regression Methods. Acta Imeko 3:46. https://doi.org/10.21014/acta_imeko.v3i4.148

7. Kyratsis P, Tzotzis A, Davim JP (2023) Experimental and 3D Numerical Study of AA7075-T6 Drilling Process. In: 3D FEA Simulations in Machining. Springer International Publishing, Cham, pp 63–75

8. Tzotzis A, Markopoulos A, Karkalos N, Kyratsis P (2020) 3D finite element analysis of Al7075-T6 drilling with coated solid tooling. In: MATEC Web of Conferences. pp 1–6

9. Tzotzis A, García-Hernández C, Huertas-Talón J-L, Kyratsis P (2020) FEM based mathematical modelling of thrust force during drilling of Al7075-T6. Mech Ind 21:415. https://doi.org/10.1051/meca/2020046

10. Tapoglou N, Efstathiou C, Tzotzis A, Kyratsis P (2023) Study of the Topography of Face Milled Surfaces Using CAD-Based Simulation. In: Kyratsis P, Manavis A, Davim JP (eds) Computational Design and Digital Manufacturing. Springer International Publishing, Cham, pp 159–166

11. Ranganathan S, Senthilvelan T, Sriram G (2010) Evaluation of Machining Parameters of Hot Turning of Stainless Steel ( Type 316 ) by Applying ANN and RSM Evaluation of Machining Parameters of Hot Turning of Stainless Steel (Type 316) by Applying ANN and RSM. Mater Manuf Process 25:1131–1141. https://doi.org/10.1080/10426914.2010.489790

12. Ghosh G, Mandal P, Mondal SC (2019) Modeling and optimization of surface roughness in keyway milling using ANN, genetic algorithm, and particle swarm optimization. 1223–1242

13. Mia M, Dhar NR (2016) Prediction of surface roughness in hard turning under high pressure coolant using Artificial Neural Network. Measurement 92:464–474. https://doi.org/10.1016/j.measurement.2016.06.048

14. Moré JJ (1978) The Levenberg-Marquardt algorithm: Implementation and theory. In: Watson GA (ed) Numerical Analysis. Springer Berlin Heidelberg, Berlin, Heidelberg, pp 105–116

15. Tzotzis A, García-Hernández C, Huertas-Talón J-L, Kyratsis P (2020) Influence of the Nose Radius on the Machining Forces Induced during AISI-4140 Hard Turning: A CAD-Based and 3D FEM Approach. Micromachines 11:798. https://doi.org/10.3390/mi11090798

16. Tzotzis A, Kakoulis K, Efkolidis N, Kyratsis P (2022) RSM-based surface roughness modelling during AISI-H13 slot milling. ACTA Tech NAPOCENSIS-Series Appl Math Mech Eng 65:1417–1424

## 7 NOTATION

The following symbols are used in this paper:

$S$ = spindle speed
$V_f$ = feed
$a_p$ = depth of cut
$R_a$ = surface roughness
$R$ = model correlation coefficient
$W_i$ = ANN output layer weight
$b$ = ANN output layer bias
$H_i$ = ANN hidden neuron